JOURNAL OF SOLID STATE CHEMISTRY 17, 157–163 (1976)

# The Fe–Se System. I. Mössbauer Spectra and Electrical Conductivity of $Fe_{1.04}Se$

TOSHIHIDE TSUJI,* ARTHUR T. HOWE, AND NORMAN N. GREENWOOD†

*Department of Inorganic and Structural Chemistry, University of Leeds, Leeds LS2 9JT, England*

Received August 2, 1975; in revised form October 6, 1975

The Mössbauer spectrum of $Fe_{1.04}Se$ (anti-PbO structure) has been measured from 4.2°K up to the phase transition, above which the isomer shift increased due to formation of FeSe (NiAs structure). The transition temperature was consistent with the value of 731°K previously determined from heat capacity measurements. The room-temperature isomer shift of $Fe_{1.04}Se$ (0.47 mm $sec^{-1}$ relative to metallic iron) and the quadrupole splitting (0.26 mm $sec^{-1}$) conformed to the trend in the known values for $Fe_{1+x}S$ and $Fe_{1.11}Te$. At 4.2°K, the Mössbauer spectrum was not magnetically split, and the application of an external magnetic field of flux density 5 Tesla showed that there was no appreciable magnetic alignment of the Fe atoms. The electrical conductivity (ca. 200 $ohm^{-1}$ $cm^{-1}$ at 295°K) was well behaved and metallic, in contrast to the semiconductivity of $Fe_{1+x}S$ and $Fe_{1.11}Te$. $Fe_{1.04}Se$ is therefore Pauli paramagnetic. Orbital structures are proposed in which the conduction occurs in either a broad low-lying basically *s–p* band, or a broadened basically Fe 3*d* type band.

Three structural types are present in the Fe–Se system: the anti-PbO structure adopted by $Fe_{1.04}Se$, the NiAs–$CdI_2$ structure adopted in the FeSe–$Fe_3Se_4$ region, and the marcasite structure adopted by $FeSe_2$ (*1*). This paper will be concerned with the anti-PbO type phase and subsequent papers will describe work on compounds with the NiAs–$CdI_2$ structure.

The tetragonal anti-PbO structure is adopted by the sulfide phase $Fe_{1+x}S$ ($0.04 < x < 0.07$) (*2*), the selenide $Fe_{1.04}Se$, where the range of homogeneity is small and uncertain (*3–8*), and the telluride phase $Fe_{1+x}Te$ ($0.11 < x < 0.25$) (*9*). These phases form the only characterized isostructural series of metal-excess chalcogenides of any transition metal. They thereby provide an attractive series for comparative magnetic and electrical conductivity studies, especially since available evidence suggests that $Fe_{1+x}S$ is a diamagnetic semiconductor (*10–12*), whereas $Fe_{1+x}Te$ is an antiferromagnetic semiconductor (*13–15*), with a Néel point of 63°K. Electrical conductivity, magnetic, and Mössbauer data for $Fe_{1.04}Se$ are lacking, although there is indirect evidence to suggest that the phase is not ferro- or strongly ferrimagnetic (*5*). We have used the Mössbauer technique primarily to investigate the magnetic behavior of the selenide, taking advantage of the fact that small quantities of ferromagnetic impurities such as Fe, or ferrimagnetic impurities such as $Fe_7Se_8$ or $Fe_3O_4$ will not swamp the Mössbauer response of the bulk material, as they can in normal susceptibility measurements. On the basis of the magnetic and electrical conductivity data we have proposed two possible orbital schemes for the selenide.

In the anti-PbO structure the metal atoms occupy two-dimensional square networks of tetrahedrally coordinated sites within the cubic close-packed anion lattice, as illustrated

* On leave from the Department of Nuclear Engineering, Nagoya University, Japan.

† Author to whom correspondence should be addressed.

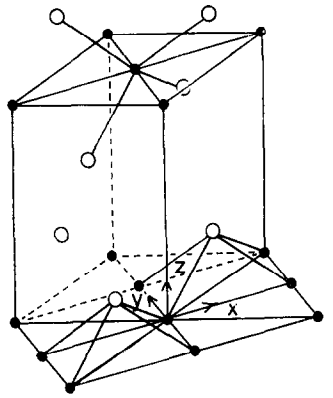


FIG. 1. Anti-PbO structure of $Fe_{1.04}Se$, showing the planar square network of Fe atoms (solid circles) and selenium atoms (open circles).

in Fig. 1. Despite the size of the chalcogens, each metal atom has four neighboring metal atoms at a distance that is larger than that in elemental α-Fe by only 3, 5.5, and 7% in the sulfide, selenide, and telluride, respectively. Both the layer-like arrangement of metal atoms and their proximity to each other might be expected to influence the magnetic and electrical properties of these compounds. The excess metal atoms ($x$) occupy some of the same octahedral positions that are found in the more metal-rich $Fe_2As$ structure (*3*, *4*).

$Fe_{1+x}S$ and $Fe_{1.04}Se$ decompose on heating at 410°K (*16*) and 731°K (*8*), respectively, into α-Fe and the stoichiometric compound with the NiAs structure, and we have investigated the transition of the selenide by means of high-temperature Mössbauer spectroscopy.

## Experimental

The samples were prepared from Johnson Matthey specpure Fe and Se. The elements were reduced in hydrogen and placed in the individual arms of a W-shaped silica tube, and the Fe was reduced for a second time in purified hydrogen at 630°K for 1 day and 1270°K for 1 day. The Fe was then magnetically transferred in the Se section, which was then sealed under hydrogen at a pressure of 13 Pa (0.1 Torr), double sealed in a larger tube and heated at 870°K for 1 day, and melted at 1350°K for 3 days with a flow of hydrogen through the furnace. The product was cooled slowly and samples for conductivity measurements were annealed for up to 2 weeks below the transition temperature. X-ray powder diffraction measurements on $Fe_{1.04}Se$ gave unit cell dimensions of $a = 376.4$ and $c = 548.6$ pm, in good agreement with those reported earlier (*8*).

Most of the Mössbauer experiments were done on a sample with an overall Fe/Se ratio of 1.09 to ensure a composition at the phase boundary with Fe. The iron in the sample was enriched to 10% in $^{57}Fe$. To prevent surface oxidation, the capsules were broken open and the ingot ground under deoxygenated hexane. Samples for the low-temperature Mössbauer measurements were made up in Apiezon grease to 10 mg (Fe) $cm^{-2}$. The high-temperature Mössbauer sample [40 mg (Fe) $cm^{-2}$] was loaded under hexane into a flat thin-walled silica capsule which was sealed under 0.1 Torr hydrogen, and the entire capsule was placed in the isothermal region of a Ricor Mössbauer furnace. The furnace was dynamically pumped at high temperature and was controlled to within 0.3°K by a Ricor TC 4B controller. Spectra were collected using a 25 mCi $^{57}Co/Rh$ source, a Harwell proportional counter and a Northern Scientific NS900 multichannel analyser synchronized to the triangular waveform of an Exeter-type generator (*17*) coupled to a Goodman transducer. The spectra were folded before computing. The isomer shifts are quoted relative to iron metal at 295°K.

For the conductivity measurements 10 g samples were prepared, and blocks 14 × 8 × 4 mm were ground under deoxygenated hexane from the dense and somewhat polycrystalline solidified melt. The four probes of copper wire were tightly wound around in grooves cut in the sample. The measurements were made over a range of currents in a hydrogen atmosphere.

## Results and Discussion

### *Mössbauer Spectra*

The most noticeable feature of the Mössbauer spectra was the complete absence of any magnetic splitting at 4.2°K, as can be seen from Fig. 2, indicating the absence of magnetic ordering. The application of a magnetic field

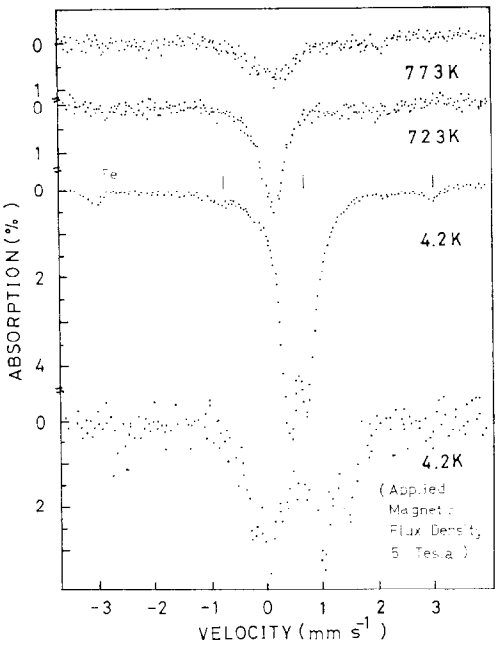


FIG. 2. Mössbauer spectra of Fe/$Fe_{1.04}Se$ from 4.2 to 723°K. At 773°K, above the phase transition, the spectrum is that of FeSe (NiAs structure) and Fe. The high-resolution spectrum at 4.2°K shows four of the six lines of α-Fe with which the $Fe_{1.04}Se$ is at equilibrium. Calculations showed that no enhancement of the applied magnetic field occurred at the Fe nuclei (bottom spectrum).

of flux density 5 Tesla did not produce an internally enhanced magnetic field at the nucleus such as would be expected if a normal paramagnetic moment existed on the Fe atoms, and the spectrum shown in Fig. 2 is consistent with the applied flux density at the nucleus of only 5 Tesla. Similar behavior was found for $Fe_{1+x}S$ (*11*) and indicates either that the compounds are low spin and diamagnetic, or that they possess Pauli (band) paramagnetism, for which the moment would be too small to be detected in the applied-field experiment.

This is the first report of the isomer shift (δ) of tetrahedrally coordinated Fe in a selenide, and the room-temperature value is compared with those of the corresponding sulfide and telluride in Table I. The values are well below those found for oxides (*18*) because of the marked covalent character of the bonding. The temperature dependence of the isomer shift, which can be seen as a shift

TABLE I

MÖSSBAUER PARAMETERS AT ROOM TEMPERATURE FOR TETRAGONAL IRON CHALCOGENIDES

| | Isomer shift (mm $sec^{-1}$)[a] | Quadrupole splitting (mm $sec^{-1}$) | Reference |
|---|---|---|---|
| $Fe_{1+x}S$ | 0.35–0.37 | — | *10, 12* |
| $Fe_{1.04}Se$ | 0.47 | 0.26 | this work |
| $Fe_{1.11}Te$ | 0.45–0.48 | 0.26 | *14, 19* |

[a] Relative to metallic iron.

towards lower values in the spectra shown in Fig. 2, is plotted in Fig. 3. Unlike the sulfide (*10*), the values for the selenide only become linear with temperature (in accordance with the high-temperature limit of the second-order Doppler shift (*18*)) at about 300°K, and this reflects the increase in mass in going from the sulfide to the selenide. The values for the telluride do not become linear until about 400°K (*19*). Hence, while we can legitimately compare isomer shifts of the sulfide and selenide, we would expect the room-temperature value for the telluride to be anomalously low. This is indeed observed in the values shown in Table I, and the series therefore effectively shows a similar increase in isomer shift from the sulfide to the telluride as does

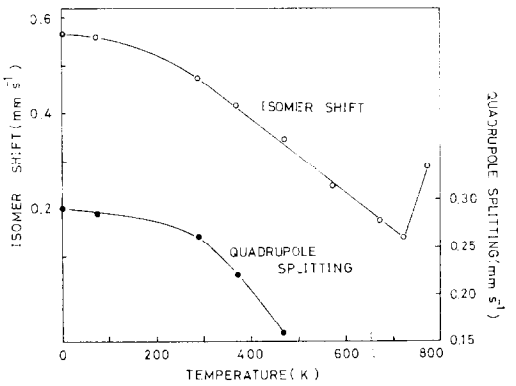


FIG. 3. Isomer shift and quadrupole splitting of $Fe_{1.04}Se$ as a function of temperature up to 723°K. The sudden increase in the isomer shift at 773°K is due to the transformation from low-spin tetrahedral Fe(II) in $Fe_{1.04}Se$ to high-spin octahedral Fe(II) in FeSe.

the only other comparable isostructural series consisting of the marcasite type $FeS_2$, $FeSe_2$, and $FeTe_2$ ($\delta = 0.28, 0.40$, and 0.47 mm $sec^{-1}$, respectively) (*20*).

The value of the isomer shift of $Fe_{1.04}Se$ of 0.47 mm $sec^{-1}$ at 295°K is lower than the value of 0.65–0.70 mm $sec^{-1}$ reported for Fe(II) in the octahedral sites of $Fe_7Se_8$ (*21*, *22*). A slightly larger difference between tetrahedrally and octahedrally coordinated Fe(II) is found in the comparable sulfides, where $\delta = 0.35$–0.37 mm $sec^{-1}$ for the tetrahedral sites of $Fe_{1+x}S$ (*10*, *12*) compared to 0.64–0.69 mm $sec^{-1}$ for the octahedral sites of $Fe_7S_8$ (*23*, *24*). An even greater difference exists when the comparison is made with FeS ($\delta = 0.76$–0.77 mm $sec^{-1}$) (*23*, *25*). These differences arise firstly from the change in coordination, which increases the *s*-electron density at the nucleus because of a higher proportion of *s* character in the bonds in going from octahedral to tetrahedral coordination, and secondly from similar changes in going from nonparamagnetic Fe(II) in $Fe_{1+x}S$ and $Fe_{1.04}Se$ to high-spin Fe(II) in FeS, $Fe_7S_8$, and $Fe_7Se_8$. This is demonstrated by the higher isomer shifts of high-spin tetrahedral Fe(II) found in $Cu_2FeSnS_4$ ($\delta = 0.57$ mm $sec^{-1}$) (*26*) and $(ZnFe)S_2$ ($\delta = 0.69$ mm $sec^{-1}$) (*27*) compared to that in nonparamagnetic $Fe_{1+x}S$ ($\delta = 0.35$–0.37 mm $sec^{-1}$).

From the discontinuity of the isomer shift between 723 and 773°K (see Figs. 2 and 3) we were able to show that the phase transition to α-Fe and FeSe was consistent with Grønvold's value of 731°K (*8*) and that it did not occur at 623°K as originally proposed by Hirone (*5*). From Fig. 2, it can be seen that at 773°K the spectrum has broadened considerably, resulting in a much smaller absorption. This may be due to diffusional broadening similar to that found in $Fe_3Se_4$ (*28*). Also the isomer shift has increased compared to the value at 723°K. Because of the reduction in intensity at 773°K, impurity peaks due to $Fe_2SiO_4$ formed by reaction of the silica with residual oxygen through an iron oxide intermediate had to be taken into account in the computer fit, and four peaks of equal halfwidth and intensity at the initial velocities reported for $Fe_2SiO_4$ (*29*) were included in the fit. The resultant isomer shift of the selenide is plotted in Fig. 3, and confirms the expected increase in going from tetrahedral Fe(II) to high-spin octahedral Fe(II). The value is slightly higher than that of $Fe_3Se_4$ at the same temperature (0.25 mm $sec^{-1}$) (*28*), as would be expected by analogy with the sulfide series FeS to $Fe_7S_8$ referred to earlier.

The small value of the quadrupole splitting implies a small deviation from cubic symmetry of the *d* (and possibly *p*) electrons in the orbitals around the Fe. The quadrupole splitting diminishes as the temperature is raised, as can be seen from Fig. 3, possibly due to thermal population of higher spin–orbit levels or to changes in the lattice contribution. In such a covalent-metallic compound, where the formal charges on the Fe and Se atoms will be very low, and where the tetrahedron of selenium atoms is only very slightly tetragonally distorted, it would be unlikely that there would be a large lattice contribution to the electric field gradient (EFG), thus ruling out the possibility of the lattice and valence terms being large and of opposite sign to produce a small net effect. The observed quadrupole splitting of 0.29 mm $sec^{-1}$ at 4.2°K is only about one-tenth of that produced by a single $3d$ electron (*18*) and the implications of this in terms of orbital configurations will be discussed later.

The asymmetry of the peaks evident in the spectrum at 4.2°K (see Fig. 2) was reduced to some extent by grinding the sample with an excess of boron nitride to prevent preferred orientation. It is likely that the residual asymmetry derived from the unresolved contribution of the 4% excess octahedral Fe atoms.

*Electrical Conductivity*

Figure 4 shows the temperature dependence of the resistivity of $Fe_{1.04}Se$; this is positive and characteristic of a well-behaved metal, in contrast to the semiconductivity reported for $Fe_{1+x}S$ (*10*) and $Fe_{1.11}Te$ (*14*).

Several precautions were taken to ensure that our measurements were characteristic of $Fe_{1.04}Se$ and were not influenced by other phases. Firstly, the ingot prepared from the melt at high temperature was not ground into a powder, but was measured intact so as to eliminate the possibility of the results being affected by surface contamination or oxidation. Such a possibility has been suggested by

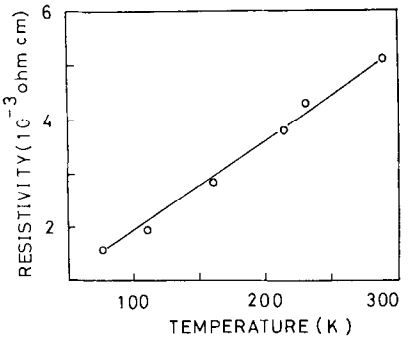


FIG. 4. Resistivity of $Fe_{1.04}Se$ as a function of temperature.

Hulliger (*30*) in order to explain the unexpected semiconductivity reported for $Fe_{1+x}S$ (*10*).

Secondly, the effect of the annealing time and the Fe/Se ratio was investigated. The Mössbauer spectra of samples annealed for different times below the transition temperature of 731°K showed that the transformation was substantially complete in a few hours. The annealing times of 10–14 days used for the conductivity samples were therefore more than adequate. The transformation from stoichiometric FeSe to $Fe_{1.04}Se$ would probably proceed via the initial formation of an intergrown matrix of $Fe_{1.04}Se$ and $Fe_{1-x}Se$. If metallic iron were present before the transformation the $Fe_{1-x}Se$ would subsequently dissolve, losing selenium to the iron and leaving a pure $Fe_{1.04}Se$ phase, possibly still with excess metallic iron in isolated regions. We compared the electrical conductivity of samples with an Fe/Se ratio of 1.12 annealed for 10 days at 570°K with that of the sample of Fe/Se ratio 1.04 annealed for 14 days at 630°K, and found that the conductivity was unchanged within the experimental limits, eliminating the possibility of any contribution from the iron phase regions, since metallic iron has a room-temperature conductivity nearly 2 orders of magnitude higher than the present values. The ratio of the conductivity at 77°K to that at 285°K was 2.85 and 3.10 for the samples with an Fe/Se ratio of 1.12 and 1.04, respectively.

If selenium were in excess, $Fe_{1-x}Se$ would remain intergrown with the $Fe_{1.04}Se$. A sample having an Fe/Se ratio of 0.96 was annealed at 570°K for 10 days and exhibited a room temperature conductivity approximately six times that of the previous samples, and the aforementioned conductivity ratio was now 1.28. This effect is attributable to conductivity via the intergrowths of $Fe_{1-x}Se$, which has a room-temperature conductivity several orders of magnitude larger than that of $Fe_{1.04}Se$. (*31*) and has a conductivity ratio of approximately 1.1, which, being lower than those previously described, indicates that the conductivity of $Fe_{1.04}Se$ has a larger metallic-like temperature coefficient than $Fe_{1-x}Se$. This confirms the conclusion that $Fe_{1.04}Se$ is indeed metallic.

*Bonding and Orbital Structure*

From the presence of metallic conductivity and the lack of any appreciable magnetic moment even in the presence of an applied field we can conclude that $Fe_{1.04}Se$ is Pauli paramagnetic rather than diamagnetic or Curie–Weiss paramagnetic. Therefore, we can deduce that the Fermi level at 0°K lies within a partly filled band and that the band or bands containing the Fermi level are broad enough to prevent correlation effects from resulting in ferro- or antiferromagnetic behavior (*32*).

The results can be interpreted by either of the orbital schemes shown in Fig. 5. The broad lower and upper bands in each case have basically $(s$–$p)$ and $(s$–$p)^*$ character, respectively, and in addition the Se 4*d* orbitals overlap with the $(s$–$p)^*$ band. In the case of the layer structure of $Fe_{1.04}Se$, the Se–Se interactions, which are included within these two bands, must account for bonding between adjoining layers of Se atoms. There is no crystallographic evidence for localized 2-centered Se–Se bonding, and each Se must bond equally with the three neighbors in the adjoining layer, as well as with the other 9 Se atoms in the close-packed structure. The Se–Se interactions might well be stabilized by admixture of the empty Se 4*d* orbitals with the Se 4*s* and 4*p* valence orbitals, and we have therefore included the 4*d* orbitals of Se in the bonding scheme.

Of the two *d* orbitals of Fe that are stabilized by the tetrahedral field, the $d_{x2-y2}$ orbital overlaps directly with the $d_{x2-y2}$ orbitals of the four close Fe neighbors, as illustrated in Fig. 1 while the $d_{z2}$ orbital remains nonbonding and localized.

The $d_{xy}$, $d_{xz}$, and $d_{yz}$ orbitals will be broadened by the antibonding interactions with the

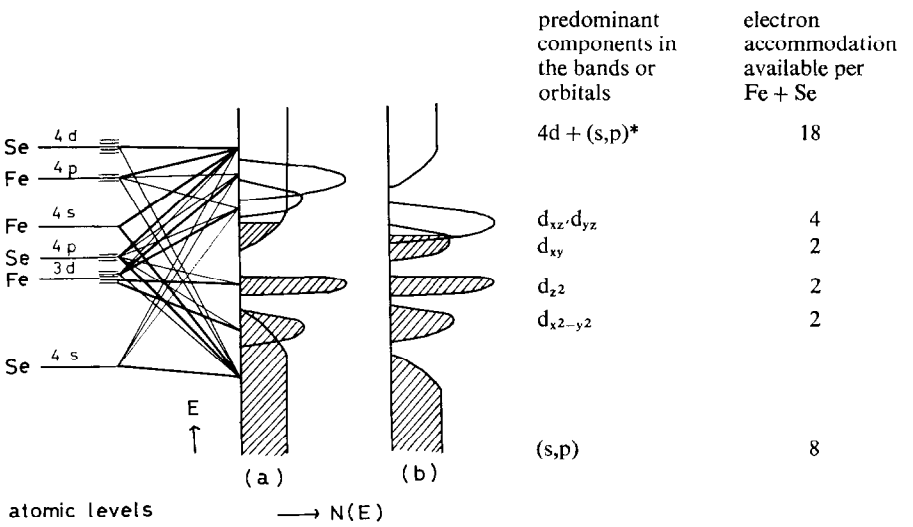


FIG. 5. Possible schematic orbital structures for $Fe_{1.04}Se$. The predominant component atomic orbitals are indicated by the heavy lines on the left of the figure. The orbitals are occupied by 14 valence electrons per Fe plus Se. The levels arising from the 4% supernumerary iron atoms in octahedral sites are not shown.

Se *s* and *p* orbitals, and in addition the $d_{xy}$ orbital will be lowered in energy by overlap with the $d_{xy}$ orbitals on the eight neighboring Fe atoms in the layer. There are a total of 14 valence electrons, of which 8 fill the valence band, 2 the $d_{x2-y2}$ orbital and 2 the $d_{z2}$ orbital, leaving 2 to occupy the upper orbitals.

The scheme shown in Fig. 5a is consistent with metallic conductivity and Pauli paramagnetism since two electrons partly fill the broad $(s–p)^*$ conduction band. The upper 3*d* orbitals lie above the bottom of this band and are unfilled. The scheme is therefore independent of the width of the 3*d* bands, and nicely explains the small observed quadrupole splitting since the filled set of $d_{x2-y2}$ and $d_{z2}$ orbitals generate no net EFG, apart from that provided by small differences in the spatial distribution of the orbitals due to delocalisation.

Alternatively, as in Fig. 5b, metallic conductivity and Pauli paramagnetism could arise if the upper 3*d* bands were both reasonably wide and overlapping and were below the bottom of the $(s–p)^*$ band. Two electrons would now partially fill the upper 3*d* bands. In this case, the small quadrupole splitting would be favoured both by significant overlap and delocalisation of the $d_{xy}$, $d_{xz}$, and $d_{yz}$ orbitals.

Consideration of the orbital structure shows that the 4% of supernumerary Fe atoms on octahedral sites could only render an otherwise semiconducting material metallic if (i) they formed a broad degenerate band system, and (ii) the $d_{xy}$ band was separated from the $d_{xz}$, $d_{yz}$ bands sufficiently for the degenerate band to be inserted without significant overlap.

The splitting of the $d_{xy}$ band from the others is unlikely to be so large, thereby disfavoring this explanation.

Both schemes illustrated in Fig. 5 therefore offer a satisfactory explanation of the observed physical properties of $Fe_{1.04}Se$. The relative positions of the $(s–p)^*$ and upper *d* bands is a matter of speculation which has been noted in many other transition-metal chalcogenides and pnictides (*1*, *33*, *34*). A possible experiment to distinguish between the two models would be to look for anisotropy in the electrical conductivity of a single crystal of $Fe_{1.04}Se$. In the particular layer structure of $Fe_{1.04}Se$, the absence of anisotropy would imply that scheme (*a*) is the correct one, since the upper 3*d* orbitals do not extend between the layers. Difficulty in achieving single-crystal growth

below the phase transition has so far prevented us from performing this measurement.

A comparison with $Fe_{1.11}Te$ shows that for this compound semiconductivity is exhibited above the Néel temperature of 63°K, while immediately below this temperature there is a small increase in the conductivity (*14*), possibly associated with the crystallographic distortion occurring at the Néel temperature (*15*). At lower temperatures, the conductivity continues to increase slowly, which may be associated with the effect of magnetic order on the conductivity (*14*). An acceptable bonding scheme for the telluride has not yet been advanced, and one which accounts for the observed properties does not immediately follow from the schemes proposed for the selenide.

The orbital schemes discussed could account for either metallic or semiconducting behavior in the sulfide $Fe_{1+x}S$. The observed semiconductivity could arise if the $d_{xy}$ band was separated from the $d_{xz}$ and $d_{yz}$ bands by stronger metal–metal interactions. The orbital scheme proposed by Kjekshus *et al.* (*12*) places 10 valence electrons around each sulfur (electron pair bonds to four Fe atoms and a lone pair) leaving only four electrons per Fe atom. Such a model is misleading for these compounds, since the number of electrons around each atom taken individually do not have to be integral, and the present band models account more naturally for the observed electrical and magnetic properties.

## References


1. F. JELLINEK, *in* "M.T.P. International Review of Science" (D. W. Sharp, Ed.), Vol. 5, Part 1, Butterworths, London (1972).
2. S. TAKENO AND A. H. CLARK, *J. Sci. Hiroshima Univ. Ser.* **C5**, 287 (1967).
3. G. HÄGG AND A. L. KINDSTRÖM, *Z. Physik. Chem.* **B22**, 453 (1933).
4. H. HARALDSEN AND F. GRØNVOLD, *Tidsskr. Kjemi Bergresen Met.* **10**, 98 (1944).
5. T. HIRONE, S. MAEDA, AND N. TSUGA, *J. Phys. Soc. Japan* **9**, 497 (1954).
6. T. HIRONE AND S. CHIBA, *J. Phys. Soc. Japan* **11**, 666 (1956).
7. F. GRØNVOLD AND E. F. WESTRUM, JR., *Acta Chem. Scand.* **13**, 241 (1959).
8. F. GRØNVOLD, *Acta Chem. Scand.* **22**, 1219 (1968).
9. F. GRØNVOLD, H. HARALDSEN, AND J. VIHOVDE, *Acta Chem. Scand.* **8**, 1927 (1954).
10. E. F. BERTAUT, P. BURLET, AND J. CHAPPERT, *Solid State Commun.* **3**, 335 (1965).
11. D. J. VAUGHAN AND M. S. RIDOUT, *J. Inorg. Nucl. Chem.* **33**, 741 (1971).
12. A. KJEKSHUS, D. G. NICHOLSON, AND A. D. MUKHERJEE, *Acta Chem. Scand.* **26**, 1105 (1972).
13. I. TSUBOKAWA AND S. CHIBA, *J. Phys. Soc. Japan* **14**, 1120 (1959).
14. E. HERMON, R. D. NOLAND, AND S. SHTRIKMAN, *Isr. J. Chem.* **9**, 1 (1971).
15. D. FRUCHART, P. CONVERT, P. WOLFERS, R. MADAR, J. P. SENATEUR, AND R. FRUCHART, *Mat. Res. Bull.* **10**, 169 (1975).
16. J. C. WARD, *Rev. Pure App. Chem.* **20**, 175 (1970).
17. P. E. CLARK, A. W. NICHOL, AND J. S. CARLOW, *J. Sci. Instrum.* **44**, 1001 (1967).
18. N. N. GREENWOOD AND T. C. GIBB, "Mössbauer Spectroscopy," Chapman and Hall, London (1971).
19. P. COFFIN, B. E. F. FENDER, AND A. T. HOWE, unpublished results.
20. A. A. TEMPERLY AND H. W. LEFEVRE, *J. Phys. Chem. Solids* **27**, 85 (1966).
21. H. N. OK AND S. W. LEE, *Phys. Rev.* **B8**, 4267 (1973).
22. C. BOUMFORD AND A. H. MORRISH, *Phys. Stat. Sol.* **22A**, 435 (1974).
23. S. HAFNER AND M. KALVIUS, *Zeit. fur Krist.* **123**, 443 (1966).
24. L. M. LEVINSON AND D. TREVES, *J. Phys. Chem. Solids* **29**, 2227 (1968).
25. R. C. THIEL AND C. B. VAN DEN BERG, *Phys. Stat. Sol.* **29**, 837 (1968).
26. N. N. GREENWOOD AND H. J. WHITFIELD, *J. Chem. Soc. (A)* 1697 (1968).
27. A. S. MARFUNIN AND A. R. MKITCHYAN, *Geochem. Internat.* **4**, 980 (1967).
28. T. TSUJI, A. T. HOWE, AND N. N. GREENWOOD, to appear.
29. M. EIBSCHÜTZ AND U. GANIEL, *Solid State Commun.* **5**, 267 (1967).
30. S. HULLIGER, "Structure and Bonding," (C. K. Jørgensen *et al.*, Ed.), Vol. 4, Springer-Verlag, Berlin (1968).
31. J. SERRE AND R. DRUILHE, *Comp. Rend. B* **262**, 639 (1966).
32. J. B. GOODENOUGH, "Magnetism and the Chemical Bond," Interscience, New York (1963).
33. N. F. MOTT, "Metal-Insulator Transitions," Taylor and Francis, London (1974).
34. J. B. GOODENOUGH, *J. Solid State Chem.* **3**, 26 (1971).